NATIONAL ADVISORY COMMITTEE FOR AERONAUTICS

WARTIME REPORT

ORIGINALLY ISSUED

January 1944 as
Advance Restricted Report 4A06

A THEORETICAL INVESTIGATION OF THE ROLLING OSCILLATIONS OF AN AIRPLANE WITH AILERONS FREE

By Doris Cohen

Langley Memorial Aeronautical Laboratory
Langley Field, Va.

NACA

WASHINGTON

NATIONAL ADVISORY COMMITTEE FOR AERONAUTICS

ADVANCE RESTRICTED REPORT

A THEORETICAL INVESTIGATION OF THE ROLLING OSCILLATIONS OF AN AIRPLANE WITH AILERONS FREE

By Doris Cohen

SUMMARY

An analysis is made of the stability of an airplane with ailerons free, with particular attention to the motions when the ailerons have a tendency to float against the wind. The present analysis supersedes the aileron investigation contained in NACA Report No. 709. The equations of motion are first written to include yawing and sideslipping, and it is demonstrated that the principal effects of freeing the ailerons can be determined without regard to these motions. If the ailerons tend to float against the wind and have a high degree of aerodynamic balance, rolling oscillations, in addition to the normal lateral oscillations, are likely to occur. On the basis of the equations including only the rolling motion and the aileron deflection, formulas are derived for the stability and damping of the rolling oscillations in terms of the hinge-moment derivatives and other characteristics of the ailerons and airplane. Charts are also presented showing the oscillatory regions and stability boundaries for a fictitious airplane of conventional proportions. The effects of friction in the control system are investigated and discussed.

If the ailerons tend to trail with the wind, the condition for stable variation of stick force with aileron deflection is found to determine the amount of aerodynamic balance that may be used. If the ailerons tend to float against the wind, the period and damping of the rolling oscillations are found to be satisfactory (in a mass-balanced system) so long as the restoring moment is not completely balanced out. Unbalanced mass behind the hinge, however, has an unfavorable effect on the damping of the oscillations and so shifts the boundary that close aerodynamic balance may not be attainable. It is found that friction may retard somewhat the damping of the aileron-free oscillations but in no case causes undamped oscillations if the ailerons are otherwise stable.

INTRODUCTION

The problem of the stability of an airplane with ailerons free has been treated in reference 1 as an adjunct to the investigation of elevator- and rudder-free motions. More recent developments in aileron design have led to an increased interest in the possible effects of positive floating tendency, that is, a tendency for the ailerons to move downward as the angle of attack is increased. Oscillations observed in flight have been thought to arise from this condition and have suggested the present more thorough investigation, in which particular attention is given to the motions when the floating tendency is positive. The present analysis is intended to supersede completely the aileron investigation of reference 1.

In the present analysis the equations of motion are first written to include all lateral degrees of freedom — sideslipping, yawing, and rolling — and movement of the ailerons. A numerical example is then used to show that the important information concerning the motions can be obtained by investigation of the rolling and aileron motions alone, although a somewhat modified interpretation of the results may be indicated. Because most ailerons are mass-balanced about the hinge axis to avoid flutter, the mass-moment parameter representing the effect of rolling acceleration on the aileron position is also omitted from the bulk of the analysis. With these simplifications it then becomes possible to derive, in terms of the remaining aileron and airplane characteristics, general formulas for the rate of damping of the oscillations, where oscillations exist, and equations expressing the conditions for stability. The hinge-moment characteristics of the ailerons will be considered the principal variables.

Charts will be presented to show numerical results in certain cases. In these examples the effects of the mass characteristics of the ailerons, which cannot readily be expressed in general formulas, will be investigated. A discussion of the effect of friction in the control system will also be included.

SYMBOLS

Airplane characteristics:

m	mass of airplane
k_X	radius of gyration of airplane about airplane X-axis
k_Z	radius of gyration of airplane about airplane Z-axis
b	wing span
c	mean wing chord
S	wing area
A	wing aspect ratio (b^2/S)
Λ	wing dihedral, radians

Aileron characteristics:

m_a	mass of aileron system
k_a	effective radius of gyration of aileron system about hinge axis
$\bar{x}$	distance from aileron center of gravity to hinge axis (positive when center of gravity is behind hinge)
$\bar{y}$	distance from aileron center of gravity to plane of symmetry of airplane
$\bar{y}'$	spanwise distance used in computing C_h to include the effect of rolling; thus, $\frac{\bar{y}'}{b/2} = \frac{C_{h_{D\phi}}}{C_{h_a}}$
b_a	span of ailerons
$\bar{c}_a$	root-mean-square aileron chord

Symbols used in describing motions (all angles are in radians):

g	acceleration of gravity
ρ	density of air
q	dynamic pressure $\left(\frac{1}{2}\rho V^2\right)$
V	steady-flight speed
s	distance along flight path
P	distance along flight path traversed during one oscillation, semispans $\left(\frac{2\pi}{n}\right)$
v	sideslip velocity (positive to right)
α	angle of attack of wing
α_e	effective angle of attack due to flap deflection
β	angle of sideslip (positive when sideslipping to right)
ψ	angle of yaw (positive when nose turns to right)
ϕ	angle of roll (positive when right wing is down)
δ	total angle of aileron deflection (positive with right wing down)
p	rolling velocity $(d\phi/dt)$
r	yawing velocity $(d\psi/dt)$
Y	side force (positive to right)
N	yawing moment
L	rolling moment in rolling-moment coefficient; lift in lift coefficient
H	hinge moment

Nondimensional quantities:

$\mu = \frac{m}{S\rho b}$ airplane density parameter

$I_X = \frac{m}{S\rho b}\left(\frac{k_X}{b/2}\right)^2$ airplane moment of inertia about X-axis

$I_Z = \frac{m}{S\rho b}\left(\frac{k_Z}{b/2}\right)^2$ airplane moment of inertia about Z-axis

$I_a = \frac{m_a}{\rho \bar{c}_a^{\,2} b_a}\left(\frac{k_a}{b/2}\right)^2$ aileron moment of inertia about hinge axis

$\xi = \frac{\partial H/\partial D^2\phi}{q\bar{c}_a^{\,2} b_a}$ mass-moment parameter, hinge axis (Nondimensional expression for effect of inertia of aileron system in causing aileron deflection when airplane is accelerated in roll.) For ailerons alone,

$$\frac{\partial H}{\partial D^2\phi} = -m_a \frac{\bar{x}}{b/2}\frac{\bar{y}}{b/2} V^2$$

t_f ratio of flap chord to airfoil chord at a given section

$\hat{D} = \frac{d}{d\left(\frac{s}{b/2}\right)} = \frac{b/2}{V}\frac{d}{dt}$ differential operator. In particular, $D\phi = \frac{pb}{2V}$

λ root of stability equation

$-a$ real part of λ, proportional to rate of damping of motions

n magnitude of imaginary part of λ, proportional to frequency of oscillations

C_n yawing-moment coefficient $\left(\frac{N}{qSb}\right)$

C_l rolling-moment coefficient $\left(\frac{L}{qSb}\right)$

C_h hinge-moment coefficient $\left(\frac{H}{q\bar{c}_a^2 b_a}\right)$

C_L lift coefficient $\left(\frac{L}{qS}\right)$

C_Y side-force coefficient $\left(\frac{Y}{qS}\right)$

Subscripts attached to moment coefficients indicate the partial derivative of the coefficient with respect to the quantity denoted by the subscript. In particular,

$C_{h_\delta} = \frac{\partial C_h}{\partial \delta}$ hinge-moment coefficient due to unit aileron deflection, or restoring tendency. Restoring tendency is positive when surface is overbalanced

$C_{h_\alpha} = \frac{\partial C_h}{\partial \alpha}$ hinge-moment coefficient due to unit change in local angle of attack, or floating tendency. Floating tendency is positive when surface floats against the relative wind

$C_{h_{D\delta}} = \frac{\partial C_h}{\partial D\delta}$ hinge-moment coefficient due to unit rate of deflection of ailerons (generally the aerodynamic damping, but may include viscous friction in the control system)

$C_{l_\delta} = \frac{\partial C_l}{\partial \delta}$ rolling moment due to unit aileron deflection, or effectiveness of the ailerons in producing roll

$\left(\frac{\partial C_L}{\partial D\delta}\right)_A$ part of additional lift due to angular velocity of flap caused by acceleration of potential flow ($-T_4$ of reference 2)

$\left(\frac{\partial C_L}{\partial D\delta}\right)_B$ part of additional lift due to angular velocity of flap caused by effective increase in camber $\left(\frac{T_{11}}{2\pi}\right.$ of reference 2$)$

$\left(\frac{\partial C_h}{\partial D\delta}\right)_A$ part of hinge moment due to angular velocity of flap caused by acceleration of potential flow

$\left(\frac{-T_4\ T_{11}}{4\pi\ t_f^2}\right.$, where T_4 and T_{11} are given in reference 2$)$

$\left(\frac{\partial C_h}{\partial D\delta}\right)_B$ part of hinge moment due to angular velocity of flap caused by effective increase in camber

$\left(\frac{T_{11}\ T_{12}}{8\pi^2\ t_f^2}\right.$, where T_{11} and T_{12} are given in reference 2$)$

The variable $D\phi$ is held constant in taking the partial derivative with respect to δ or $D\delta$, which is equivalent to holding α constant.

The following symbols are adopted because of common usage:

$C_{l_p} = \frac{\partial C_l}{\partial \frac{pb}{2V}}$ aerodynamic damping of the airplane in roll

$C_{n_p} = \frac{\partial C_n}{\partial \frac{pb}{2V}}$; $C_{l_r} = \frac{\partial C_l}{\partial \frac{rb}{2V}}$; and $C_{n_r} = \frac{\partial C_n}{\partial \frac{rb}{2V}}$

ANALYSIS

Equations of Motion

The general equations of lateral motion with ailerons free, coupling the rolling motion of the airplane with the yawing and sideslipping motions and with the movements of the ailerons following a small disturbance, are as follows:

$$m(\dot{v} + V\dot{\psi}) - \beta \frac{\partial Y}{\partial \beta} - \phi mg = 0 \tag{1}$$

$$mk_Z^2 \ddot{\psi} - \dot{\psi} \frac{\partial N}{\partial \dot{\psi}} - \beta \frac{\partial N}{\partial \beta} - \dot{\phi} \frac{\partial N}{\partial \dot{\phi}} - \delta \frac{\partial N}{\partial \delta} - \dot{\delta} \frac{\partial N}{\partial \dot{\delta}} = 0 \tag{2}$$

$$mk_X^2 \ddot{\phi} - \dot{\phi} \frac{\partial L}{\partial \dot{\phi}} - \beta \frac{\partial L}{\partial \beta} - \dot{\psi} \frac{\partial L}{\partial \dot{\psi}} - \delta \frac{\partial L}{\partial \delta} - \dot{\delta} \frac{\partial L}{\partial \dot{\delta}} = 0 \tag{3}$$

$$m_a k_a^2 \ddot{\delta} - \dot{\phi} \frac{\partial H}{\partial \dot{\phi}} - \beta \frac{\partial H}{\partial \beta} - \dot{\psi} \frac{\partial H}{\partial \dot{\psi}} - \delta \frac{\partial H}{\partial \delta} - \dot{\delta} \frac{\partial H}{\partial \dot{\delta}} + \ddot{\phi} \frac{\partial H}{\partial \ddot{\phi}} = 0 \tag{4}$$

where the dot over a quantity denotes its derivative with respect to time.

For small angles of sideslip, $v = \beta V$. Dividing equation (1) by qS, equations (2) and (3) by qSb, equation (4) by $q\bar{c}_a^2 b_a$, and introducing the nondimensional operator $D = \dfrac{d}{d\left(\frac{s}{b/2}\right)}$ yields the following nondimensional equations:

$$\left.\begin{aligned}
&\left(4\mu D - C_{Y_\beta}\right)\beta - C_L\phi + 4\mu D\psi = 0 \\
&-C_{n_\beta}\beta - C_{n_p} D\phi + \left(2I_Z D - C_{n_r}\right) D\psi - \left(C_{n_{D\delta}} D + C_{n_\delta}\right)\delta = 0 \\
&-C_{l_\beta}\beta + \left(2I_X D - C_{l_p}\right) D\phi - C_{l_r} D\psi - \left(C_{l_{D\delta}} D + C_{l_\delta}\right)\delta = 0 \\
&-C_{h_\beta}\beta + \left(-\xi D - C_{h_{D\phi}}\right) D\phi - C_{h_{D\psi}} D\psi + \left(2I_a D^2 - C_{h_{D\delta}} D - C_{h_\delta}\right)\delta = 0
\end{aligned}\right\} \tag{5}$$

If solutions are assumed to have the form $Ce^{\lambda \frac{s}{b/2}}$, the exponent λ must satisfy the stability equation in D obtained by setting the determinant composed of the coefficients of β, ϕ, $D\psi$, and δ equal to zero. In the general case described by equations (5), the stability equation is of the sixth degree in λ and the six roots may indicate motions composed of as many as three oscillatory components. By means of simplifying assumptions justified by the examination of numerical examples, the stability equation will eventually be reduced to a cubic.

Preliminary Calculations

It is first proposed to simplify the analysis by neglecting the coupling between the rolling motion and the yawing and sideslipping motions. In order to test the validity of such a treatment, two sets of calculations have been made for a specific case, one set including the cross-coupling, and one set considering only the rolling and aileron motions.

Numerical values assumed.- The airplane characteristics assumed are given in table I. A lift coefficient of 1.0 was chosen to magnify any differences between the two results. The stability derivatives were obtained, with the exception of C_{l_p}, from table I of reference 3. The value of C_{l_p} was taken from reference 4, on the assumption of a 2:1 tapered wing of aspect ratio 6. The mass characteristics are intended to be representative of a conventional pursuit-type airplane.

The aileron characteristics assumed are for 15-percent-chord ailerons covering the outer 40 percent of the wing span. The values of the derivatives are listed in table II. The ailerons were assumed to be mass-balanced; consequently, $\xi = 0$. The moment of inertia of the ailerons was also taken equal to zero. (The validity of a comparison made on the basis of zero moment of inertia will be checked in a subsequent section.) The hinge-moment parameters Ch_α and Ch_δ were retained as the principal variables.

Nature of the motions, four degrees of freedom.- The composition of the motions, as indicated by the roots of the stability equation for various combinations of

C_{h_α} and C_{h_δ}, is described in figure 2. With I_a and ξ equal to zero, the stability equation for this figure is a quintic and there are, therefore, five roots to be accounted for. It is possible to consider separately one real root; this root passes through zero along a line designated in figure 2 as the spiral divergence boundary. In the region around the positive C_{h_α}-axis the remaining four roots form two complex pairs, indicating that the motions have two oscillatory components. Along the long-dashed curve one oscillation disintegrates into two aperiodic modes, divergent or convergent accordingly as the oscillations are stable or unstable; at all values of C_{h_α} and C_{h_δ} outside this curve the motion is composed of one oscillatory mode, which is almost always stable, and three nonoscillatory components. Inside the curve, the two oscillatory components are stable so long as C_{h_δ} is negative. As C_{h_δ} becomes positive, instability sets in, as indicated by the oscillatory stability boundary. In general, only one mode becomes unstable; the same oscillation breaks down into two aperiodic modes at a slightly larger value of C_{h_δ}. In a small region (AB in figure. 2) defined by the intersection of the two branches of the boundary, both modes are unstable. This detail and others occurring outside the stable region, or near the boundary, are not considered of any practical importance; they are mentioned in order to answer questions that might otherwise be suggested by inspection of the figure.

Rate of divergence, four degrees of freedom.- Inasmuch as figure 2 indicates that the motions will be unstable for most combinations of values of C_{h_α} and C_{h_δ}, it seems advisable first to examine the nature of the divergent instability, which appears almost unavoidable. The condition for neutral stability (zero root) is that the constant term of the stability equation vanish; that is,

$$C_{h_\delta}\left(C_{l_\beta}C_{n_r} - C_{l_r}C_{n_\beta}\right) + C_{h_{D\psi}}\left(C_{n_\beta}C_{l_\delta} - C_{l_\beta}C_{n_\delta}\right)$$

$$+ \lambda C_{h_\alpha}\left(C_{n_\delta}C_{l_r} - C_{l_\delta}C_{n_r}\right) = 0$$

The rate of divergence for the unstable values of C_{h_α} and C_{h_δ} (for the specific case to which fig. 2 pertains) is indicated by the lines of equal roots in figure 3. Although these lines appear to go through the origin, each has its intercept at a positive value of C_{h_δ} proportional to the value of the root. For small values of the root, however, the intercepted distance is negligible, and the loci may be considered lines of constant floating ratio $\frac{\delta}{\alpha} = -\frac{C_{h_\alpha}}{C_{h_\delta}}$. Figure 3 shows that the divergence over most of the range of negative C_{h_δ} is very slow. This divergence is, in fact, the so-called "spiral instability" that is generally anticipated by airplane designers. In the fourth quadrant, however, a sudden rapid increase in the rate of divergence is observed, which corresponds to a change of sign in the coefficient of λ in the stability equation. From the practical point of view the floating ratio at which this sudden increase occurs locates the significant "divergence boundary." A line through this region and the oscillatory stability boundary may therefore be considered the complete boundary for stability of the airplane with all four degrees of freedom.

Equations for two degrees of freedom.- The information obtained from calculations neglecting the yawing and sideslipping motions will now be considered. The equations of motion simplified to include only coupling between rolling and aileron motion are as follows (nondimensional form):

$$\left.\begin{aligned}\left(2I_X D - C_{l_p}\right)D\phi - \left(C_{l_{D\delta}}D + C_{l_\delta}\right)\delta = 0 \\ \left(-\tfrac{g}{}D - C_{h_{D\phi}}\right)D\phi + \left(2I_a D^2 - C_{h_{D\delta}}D - C_{h_\delta}\right)\delta = 0\end{aligned}\right\} \quad (6)$$

and the stability equation is

$$4I_X I_a \lambda^3 - 2\left(C_{h_{D\delta}} I_X + C_{l_p} I_a + \frac{1}{2} C_{l_{D\delta}} \xi\right)\lambda^2$$

$$+ \left(C_{l_p} C_{h_{D\delta}} - 2C_{h_\delta} I_X - C_{l_{D\delta}} C_{h_{D\phi}} - C_{l_\delta} \xi\right)\lambda$$

$$+ \left(C_{l_p} C_{h_\delta} - C_{l_\delta} C_{h_{D\phi}}\right) = 0 \qquad (7)$$

Nature of the motions, two degrees of freedom.- For the case defined by tables I and II, the motions are as described in figure 4. The stability equation is a cubic, and there is again one real root, which becomes zero at the divergence boundary. The remaining two roots form a complex pair, indicating an oscillatory mode, inside the region defined by the long-dashed curve. Outside this region all three roots are real and no oscillations occur. The oscillations become unstable at a small positive value of C_{h_δ}, which is almost independent of the value of C_{h_α}.

Comparison of results, two and four degrees of freedom.- The results of the two computations can now be tested for agreement. Comparison of figures 2, 3, and 4 suggests that the effective divergence boundary of the cross-coupled motions (shown by the dotted line in fig. 2) may be assumed to coincide with the true divergence boundary in the simplified case. Thus, where the simplified analysis indicates a change from stability to instability, there is actually a sudden transition from a slow divergence to a rapid one. The comparison may be extended into the first quadrant of the charts. Here the divergence boundary appears, in the more exact analysis, as a branch of the boundary between damped and undamped oscillations (line OA, fig. 2). The oscillations are, however, on the point of breaking down into aperiodic modes and the instability would in practice be indistinguishable from uniform divergence. In accordance with these observations the line of zero roots obtained from the simplified analysis will be termed the "divergence boundary," with the understanding that such a designation is strictly true only when the cross-coupling is negligible.

Further comparison of figures 2 and 4 shows that the oscillatory stability boundary of the simplified treatment, although shifted slightly by the introduction of the additional degrees of freedom, is so little altered that it also may be retained as part of the stability boundary. Moreover, the position of the line enclosing the oscillatory region remains essentially unchanged and still indicates the values of the hinge moments at which one oscillation breaks down. It may therefore be concluded that, except for the presence everywhere of an additional mode of oscillation to be discussed subsequently, the broad aspects of the solution for the more complex case may be deduced from the results of the simplified analysis.

Comparison of the roots at a number of points shows that the results of the two calculations are in close quantitative agreement, also, with regard to the oscillatory mode common to both analyses. Thus, both the period and the damping of the oscillations of one mode can be obtained from the results of the simplified analysis.

The oscillations of the second mode have both damping and period virtually independent of the hinge moments of the ailerons. In the case chosen for illustration the period is of the order of 30 semispans, or, if the span is 40 feet and the wing loading 40 pounds per square foot, about $3\frac{1}{2}$ seconds, throughout the range of C_{h_α} with C_{h_δ} negative; the motion damps to half amplitude in the course of one oscillation. Because the aileron characteristics are not involved and because of the magnitudes of the period and damping, this mode appears to be the normal lateral oscillation of the airplane with controls fixed and as such is treated elsewhere in the literature. For the assumed airplane this mode does not become unstable anywhere within the region indicated as stable by the simplified analysis.

Effect of aileron moment of inertia on cross-coupling.- It seems desirable to check the foregoing conclusion against results obtained with the moment of inertia of the aileron system retained in the equations. For this purpose, the roots of the stability equations have been calculated at $C_{h_\alpha} = 0.15$ and $C_{h_\delta} = 0.02$,

-0.1, -0.2, and -0.3, with $I_a = 0.025$. With four degrees of freedom, the stability equation has six roots. Of these, one root indicates the spiral mode and, in the unstable region, has the same values as are given by figure 3 for the case with zero moment of inertia. A second real root corresponds to the real root of the simplified equation. The four remaining roots form, in general, two oscillatory pairs. These roots are compared with those of the simplified equation in the following table:

C_{h_δ}	Two degrees of freedom, $I_a = 0.025$	Four degrees of freedom, $I_a = 0.025$	
0.02	-0.0037 ± 0.19i	-0.0044 ± 0.22i	-0.0246 ± 0.110i
-.1	-1.043 ± .843i	-1.053 ± .851i	-.0258 ± .199i
-.2	-1.077 ± 1.662i	-1.081 ± 1.664i	-.0245 ± .199i
-.3	-1.086 ± 2.186i	-1.083 ± 2.189i	-.0241 ± .199i

At $C_{h_\delta} = 0.02$, where the periods are of the same order of magnitude, the effect of the cross-coupling is seen. Elsewhere the period and damping in both calculations agree within 1 percent. It appears reasonable to conclude that the statements of the preceding section hold in spite of the omission of the aileron moment of inertia from the calculations.

Simplified Analysis

Using the reduced form of the stability equation makes it possible to investigate the effects on the stability of the airplane of varying the aileron characteristics, and even to give certain general formulas. Because most modern airplanes are designed with ailerons completely mass balanced, these formulas may be still further simplified by assuming ξ equal to zero.

Aileron-free oscillations.- The oscillations associated with freeing the aileron controls can now be investigated in more detail. If a pair of roots is assumed in the form $\lambda = -a \pm ni$, a relation can be derived giving the frequency n in terms of the coefficients of λ in equation (7). This relation is too lengthy to be presented in its general form; however, calculations have been made from it and the results will

be shown in the form of lines of equal period $P = 2\pi/n$ on the stability charts.

The damping of the oscillations is more readily expressible than is the period, particularly if a fixed value of the frequency is assumed. Moreover, calculations of the damping for zero frequency and for the highest frequency likely to be encountered in practice showed that the expression could be still further simplified by omitting the terms containing the frequency and C_{h_α} (since these terms apparently canceled each other) without any appreciable loss in accuracy. Thus, with ζ equal to zero, the damping a is, to a good approximation, the smaller root of the quadratic

$$3a^2 + \left(\frac{C_{h_{D\delta}}}{I_a} + \frac{C_{l_p}}{I_X}\right) a + \left(\frac{C_{l_p} C_{h_{D\delta}}}{4I_X I_a} - \frac{C_{h_\delta}}{2I_a}\right) = 0 \qquad (8)$$

which is independent of C_{h_α}.

At the stability boundary, the damping a is zero, and, therefore,

$$C_{h_\delta} = \frac{C_{l_p} C_{h_{D\delta}}}{2I_X} \qquad (9)$$

approximately.

The more accurate expression for this boundary is obtained by setting Routh's discriminant equal to zero. The result is a linear relation between C_{h_δ} and C_{h_α}; that is,

$$C_{h_\delta} = \frac{C_{l_p}}{2I_X^2}\left(C_{h_{D_\delta}} I_X + C_{l_p} I_a\right) - \left(\frac{\bar{y}'}{b/2}\right) \frac{C_{h_{D\delta}} C_{l_{D\delta}} I_X + 2C_{l_\delta} I_a I_X + C_{l_p} C_{l_{D\delta}} I_a}{2I_X^2 \, C_{h_{D\delta}}} C_{h_\alpha} \qquad (10)$$

Figure 4, however, shows the variation with C_{h_α} to be actually quite small.

Stick-force criterion.- The divergence boundary is obtained by setting the constant term of the stability equation equal to zero; then,

$$\frac{C_{h_\delta}}{C_{h_\alpha}} = \left(\frac{\bar{y}'}{b/2}\right) \frac{C_{l_\delta}}{C_{l_p}} \tag{11}$$

This condition for neutral stability is identical with the equation for zero slope of the hinge-moment curve:

$$\frac{dC_h}{d\delta} = C_{h_\delta} + \frac{dD\phi}{d\delta} C_{h_{D\phi}} = 0 \tag{12}$$

and is therefore also identified with the condition for zero stick force in pure roll or in a rapid rolling maneuver. Inasmuch as the stick force per unit deflection of the ailerons is proportional to $\frac{dC_h}{d\delta}$, lines of constant stick force are obtained by replacing the zero in equation (12) by appropriate constants. The rolling effectiveness, $\frac{dD\phi}{d\delta} = \frac{pb}{2V}$ per unit aileron deflection, is independent of the hinge moments; the equation for constant stick force therefore results in a family of straight lines parallel to the divergence boundary of equation (11) and the criterion for light stick force for given aileron dimensions and effectiveness is the closeness with which that boundary is approached. A comparison of one aileron with another, however, shows that the stick force will also be proportional to the value of $\bar{c}_a^2 b_a$.

Method of investigating the effect of friction.- When the effect of friction in the control system is considered, it is necessary to distinguish between two types, viscous friction and solid friction. Viscous friction, which varies with the speed of the flap deflection, is exactly equivalent to an increase in $C_{h_{D\delta}}$,

heretofore considered to be due only to the aerodynamic damping of the ailerons. Solid friction acts in a more complex way but may be approximated by an equivalent viscous damping, the amount varying inversely with the amplitude of the deflection. (A more detailed discussion of this approximation is given in reference 7.) Thus, in the course of a damped oscillation, for example, the apparent $C_{h_{D\delta}}$ increases and the question of the effect of the friction reduces to the question of whether an increase in $C_{h_{D\delta}}$ is stabilizing or destabilizing.

EXPLANATION OF CHARTS

The stability charts (figs. 5 to 9) are intended both as illustrations of the application of the preceding formulas and as working charts from which the behavior of a particular set of ailerons on a conventional airplane may be predicted. If the analysis is to be applied to an airplane having stability characteristics that represent a considerable departure from those tabulated herein, it will probably be advisable to calculate the nature of the motions from the general formulas (equations (7), (8), (10), and (11)).

Figures 5 to 9 show the oscillatory regions and lines of equal period in those regions, as well as the stability boundaries for aileron-free motion. (The damping of the oscillations is shown separately in fig. 10.) Figures 5, 6, and 7 show the results for 15-percent-chord ailerons with three different moments of inertia covering a wide range of values. In all other respects the ailerons are those previously used as a basis for the preliminary calculations. The airplane characteristics are those given in table I. Figures 8 and 9 present stability regions for 30-percent-chord ailerons of the same effectiveness C_{l_δ} as the 15-percent-chord ailerons of figures 5, 6, and 7. The span for the wider ailerons would be 28 percent of the wing span, as against 40 percent for the narrower ones. The other characteristics of the 30-percent-chord ailerons are listed in table II. Two values of I_a are presented for comparison. The airplane characteristics are not changed from those of table I.

In figures 5 to 9, the value used for the aerodynamic damping of the aileron motion $C_{h_{D\delta}}$ is the theoretical value for unbalanced flaps (fig. 1). The value of $C_{h_{D\delta}}$ actually varies with the amount of balance and is therefore not constant for any one chart. Moreover, the variation depends on the manner in which the balance is obtained. The variation is, however, slight in any case -- less, for example, than the amount introduced by friction. (If balancing area is added ahead of the hinge, complete balance involves approximately 15 percent reduction in $C_{h_{D\delta}}$ from the theoretical value.) The variation of $C_{h_{D\delta}}$ with C_{h_δ} and C_{h_α}, therefore, need not be incorporated into the charts. The effect of a change in $C_{h_{D\delta}}$ may be estimated by a comparison of figure 5 with figure 8, and of figure 6 with figure 9, inasmuch as the principal difference between the calculations for the narrow- and wide-chord ailerons of the same effectiveness is an increase in $C_{h_{D\delta}}$.

The relative magnitudes of the stick forces for the narrow- and wide-chord ailerons are indicated by the spacing of the lines of equal stick force in figures 5 and 8. The hinge moments are expressed in these figures in terms of the mean wing chord in order to make possible a direct comparison of actual forces. As previously noted, all the lines are parallel to the line of zero stick force, that is, to the divergence boundary.

Figure 10 shows the distance required for the oscillations to damp to one-half amplitude. This distance is $0.693/a$, where a is given by equation (8). A single value of I_a was selected, and the distance to damp to one-half amplitude was plotted against C_{h_δ} for several values of $C_{h_{D\delta}}$. The figure was designed primarily to serve as the basis for the discussion of the effect of friction and is, therefore, more general than the preceding charts. The damping for 15-percent-chord ailerons without friction is also shown, however, (to be applied to fig. 6) and the damping for 30-percent-chord ailerons, $I_a = 0.025$, (to be used with fig. 9) may be understood to coincide with the line for

$C_{h_{D\delta}} = -0.2$. The inclusion of lines for other values of I_a would not affect the conclusions to be drawn from the figure.

In figure 11 the stability boundaries are shown in the same form as in figures 5 to 9 for values of ξ varying from complete balance ($\xi = 0$) to a value roughly corresponding to that for an aileron with center of gravity 20 percent of its chord behind the hinge ($\xi = -0.6$). From equation (7) it can be seen that ξ does not enter into the stick-force criterion. Routh's discriminant, however, is derivable as an essentially linear relation between C_{h_δ} and ξ. Although the boundaries shown are for $I_a = 0.0125$, they are practically invariant with the moment of inertia. The effects of increasing the damping of the ailerons or $C_{h_{D\delta}}$ and of changing ξ are substantially additive, neither change affecting the variation of critical C_{h_δ} with the other variable. It may be generally concluded from figure 11, therefore, that the presence of unbalanced mass behind the aileron hinge restricts the permissible degree of aerodynamic balance.

DISCUSSION OF RESULTS

Oscillatory Modes

Oscillatory regions.- It may be seen from the figures that in all cases rolling oscillations (in addition to the normal lateral mode) will follow a disturbance if C_{h_δ} is small and C_{h_α} is positive. From figures 8 and 9 it may be concluded that the range of C_{h_δ} for which oscillations are possible increases with the width of the ailerons. As previously suggested, figures 8 and 9 may also be understood to indicate the increase in the extent of the oscillatory region with increased $C_{h_{D\delta}}$ due to any other cause.

Effect of I_a.- Comparison of figures 5, 6, and 7 and of figures 8 and 9 shows that the moment of inertia of the ailerons introduces a second oscillatory region. On further investigation, the oscillations in this region are found to be very rapid but well damped. Both

damping and period depend almost entirely on the tendency of the ailerons to resist deflection, as expressed by C_{h_δ}, $C_{h_{D\delta}}$, and the moment of inertia I_a (See section entitled "Effect of aileron moment of inertia on cross-coupling" for values of the roots in this region.) The motion is therefore interpreted as a flapping movement of the ailerons uncoupled with the motion of the airplane. This mode is so well damped (maximum distance to damp to half amplitude = 0.63 semispan in the range considered) as to be of no practical importance and further discussion will therefore be limited to the rolling oscillations occurring in the neighborhood of $C_{h_\delta} = 0$.

Period of the aileron-free rolling oscillations.- The period of the rolling oscillations depends to a large extent on the floating tendency of the ailerons. When $C_{h_\alpha} = -0.4$, for example, the period for narrow ailerons may be of the order of 15 semispans, or, if the airplane is traveling at 400 feet per second and has a 40-foot wing span, three-quarters of a second. In the case of wider ailerons or of ailerons with smaller positive floating tendency, the period is considerably longer.

Damping of Oscillations

It is perhaps preferable to consider the period in conjunction with the damping of the oscillations. The distance required for the oscillations to damp to half amplitude is shown in figure 10. Application of figure 10 to the preceding figures indicates that, so long as C_{h_δ} is negative, the motion damps to half amplitude in a fraction of an oscillation. If the ratio $C_{h_\delta}/C_{h_{D\delta}}$ is in the neighborhood of 0.3 or greater, the ratio of period to damping distance is so large as to make the motion in effect a uniform subsidence.

Effect of airplane characteristics.- It should be remembered that the preceding conclusions are based on computations for a particular airplane and are not quantitatively applicable in general. If the ratio of damping in roll to moment of inertia in roll C_{l_p}/I_X is numerically greater than the value of -0.4 assumed for the example, the damping of the oscillations will be

more rapid than is shown by figure 10. In addition, the boundary will be shifted to the right, with the amount of positive C_{h_δ} allowed increased proportionately to the increase in C_{l_p}/I_X (equation (9)).

With the exception of the considerable effect of unbalanced mass, shown in figure 11, no factors other than those just discussed enter critically into the damping or stability of the oscillatory mode. The effect of variations in floating tendency can be seen in figures 5 to 9, where lines of equal damping would be very nearly parallel to the oscillatory stability boundaries. The parameter C_{l_δ}, the aileron effectiveness, enters into the expression for the stability boundary (equation (10)) in combination with C_{h_α} and has similarly little influence on it. (It may be noted here that the period of the oscillation is also affected by a change in C_{l_δ} in roughly the same way as by a proportionate change in C_{h_α}.) The moment of inertia of the ailerons appears in equation (8) for the damping, acting to reduce the time required for damping to half amplitude. The effect of I_a on the position of the boundary (zero damping) is, however, negligible, as may be seen by comparing figures 5, 6, and 7, and figures 8 and 9.

Effect of Friction

The effect of viscous friction in the control system, as has been noted, is merely to augment the resistance to the aileron motion as expressed by $C_{h_{D\delta}}$. The result may be seen in the charts for increased aileron chord (figs. 8 and 9). Oscillations occur over a wider range of C_{h_δ} than with a frictionless system. Also (from fig. 10) the rate of damping is generally lower, when C_{h_δ} is negative, because of the phase lag between δ and $D\delta$; however, if C_{h_δ} is positive, the additional damping will retard the motion and extend the range of stable C_{h_δ}.

If solid friction is present, the effective value of $C_{h_{D\delta}}$ will gradually increase as the oscillations

die down -- according to the approximate theory, approaching infinity as the amplitude approaches zero, but in actual practice causing the ailerons to stick at some small angle of deflection. While this change in effective $C_{h_{D\delta}}$ is taking place, the rate of damping will slowly decrease or increase, accordingly as C_{h_δ} is negative or positive, and will approach the rate corresponding to the ailerons-fixed condition, as shown by figure 10. In no case will oscillations of increasing amplitude occur because of the presence of friction if the ailerons are otherwise stable. Moreover, because the damping approaches a finite (non-zero) rate, there is no possibility of steady oscillations, such as occur in the rudder-free condition (reference 7).

CONCLUSIONS

1. The stability of an airplane with ailerons free may be determined to a very large extent without regard to the cross-coupling between the rolling motion and the yawing and sideslipping motions. Neglecting the yawing and sideslipping leads to a simplified analysis that does not predict the occurrence of spiral instability. The simplified analysis does, however, predict the values of the hinge moments at which the instability becomes violent. Also, the simplified analysis will not include the normal lateral oscillation of the airplane with controls fixed, but the stability of this mode is not affected by freeing the ailerons and that phase of the problem is outside the scope of the present investigation.

2. Divergence, or an unstable variation of the control force with aileron deflection, is the only form of instability likely to occur in the case of mass-balanced ailerons with negative floating tendency, except for flutter, which is not considered in this analysis. The use of ailerons with considerable tendency to float against the wind, however, introduces the possibility of oscillatory motion with the ailerons free and, if the ailerons are aerodynamically overbalanced, of oscillatory instability. The unstable oscillations exist in addition to the normal rolling-yawing oscillations introduced by the dihedral angle and by the directional stability of the airplane.

3. As long as the restoring moment is not completely balanced out, the damping of the aileron-free oscillations in a mass-balanced system is so great as to make the oscillations appear to be of no practical concern. The presence of unbalanced mass behind the hinge, however, restricts somewhat the permissible degree of aerodynamic balance.

4. Comparison of the 15-percent-chord and 30-percent-chord ailerons shows that aerodynamic overbalance is permissible, from considerations of stability, in the case of shorter, wider-chord ailerons if considerable positive floating tendency is present. The permitted increase in aerodynamic balance is not enough, however, to offset the rapid increase in stick force with aileron chord. On the other hand, the oscillations are of considerably lower frequency for wide ailerons than are those that occur at the same stick force in the case of narrower ailerons.

5. The presence of viscous friction in the control system has the same effect as increasing the aerodynamic damping of the ailerons. The presence of solid friction in an otherwise stable system has the effect of gradually increasing or decreasing the damping of the oscillations as their amplitude decreases so as to cause the rate of damping with ailerons free to approach the rate with ailerons fixed. Neither instability nor steady oscillations will result from the presence of friction.

6. The stability of the control-free oscillations is virtually independent of the moment of inertia, floating tendency, or effectiveness of the ailerons.

7. An airplane with a large ratio of damping in roll to moment of inertia about the X-axis permits a closer degree of balance in the ailerons before oscillatory instability is incurred and, with ailerons free, such an airplane is generally more stable than one for which this ratio is small.

Langley Memorial Aeronautical Laboratory,
National Advisory Committee for Aeronautics,
Langley Field, Va.

REFERENCES

1. Jones, Robert T., and Cohen, Doris: An Analysis of the Stability of an Airplane with Free Controls. Rep. No. 709, NACA, 1941.

2. Theodorsen, Theodore: General Theory of Aerodynamic Instability and the Mechanism of Flutter. Rep. No. 496, NACA, 1935.

3. Jones, Robert T.: The Influence of Lateral Stability on Disturbed Motions of an Airplane with Special Reference to the Motions Produced by Gusts. Rep. No. 638, NACA, 1938.

4. Weick, Fred E., and Jones, Robert T.: The Effect of Lateral Controls in Producing Motion of an Airplane as Computed from Wind-Tunnel Data. Rep. No. 570, NACA, 1936.

5. Pearson, Henry A., and Jones, Robert T.: Theoretical Stability and Control Characteristics of Wings with Various Amounts of Taper and Twist. Rep. No. 635, NACA, 1938.

6. Munk, Max M.: Fundamentals of Fluid Dynamics for Aircraft Designers. The Ronald Press Co., 1929.

7. Greenberg, Harry, and Sternfield, Leonard: A Theoretical Investigation of the Lateral Oscillations of an Airplane with Free Rudder with Special Reference to the Effect of Friction. NACA A.R.R., March 1943.

TABLE I

AIRPLANE CHARACTERISTICS

Wing characteristics:

Taper ratio	2:1
Aspect ratio, A	6
Dihedral angle, Γ, degrees	5
Lift curve slope, C_{L_α}	4.3

Mass characteristics:

μ	12.5
$k_X/\frac{b}{2}$	0.3
I_Z	1.5

Stability derivatives:

C_{n_β}	0.067
C_{n_p}	-0.055
C_{n_r}	-0.109
C_{l_β}	-0.088
C_{l_p}	-0.450
C_{l_r}	0.250
C_{Y_β}	-0.41

TABLE II

AILERON CHARACTERISTICS

Derivative	Explanation	Value	
		15-percent-chord ailerons	30-percent-chord ailerons
C_{l_δ}	From figure 16 of reference 5, with $k = \frac{\partial \alpha_e}{\partial \delta}$ obtained from empirical curve of figure 1 herein	-0.156	-0.156
$C_{l_{D\delta}}$	$C_{l_{D\delta}} = \frac{C_{l_\delta}}{\frac{2\pi A}{A+4}} \times \frac{C_{L_{D\delta}}}{\partial \alpha_e / \partial \delta}$ (See fig. 1.)	-0.013	-0.023
C_{n_δ}	$C_{n_\delta} = -C_{l_\delta} \times \frac{3C_{L_\alpha}}{\pi A}$ (Reference 6, p. 107)	0.0248	0.0248
$C_{n_{D\delta}}$	$C_{n_{D\delta}} = -C_{l_{D\delta}} \times \frac{3C_{L_\alpha}}{\pi A}$ (Reference 6, p. 107)	0.002	0.002
$C_{h_{D\delta}}$	For frictionless system. (See fig. 1 for formula.)	-0.110	-0.220
$C_{h_{D\psi}}$	Considered negligible	0	0
$C_{h_{D\phi}}$	$C_{h_{D\phi}} = \frac{\bar{y}'}{b/2} C_{h_\alpha}$ From an unpublished analysis correlating wind-tunnel and flight-test data	0.66 C_{h_α}	0.72 C_{h_α}
C_{h_β}	$C_{h_\beta} = C_{h_\alpha} \Lambda$	0.0873 C_{h_α}	0.0873 C_{h_α}

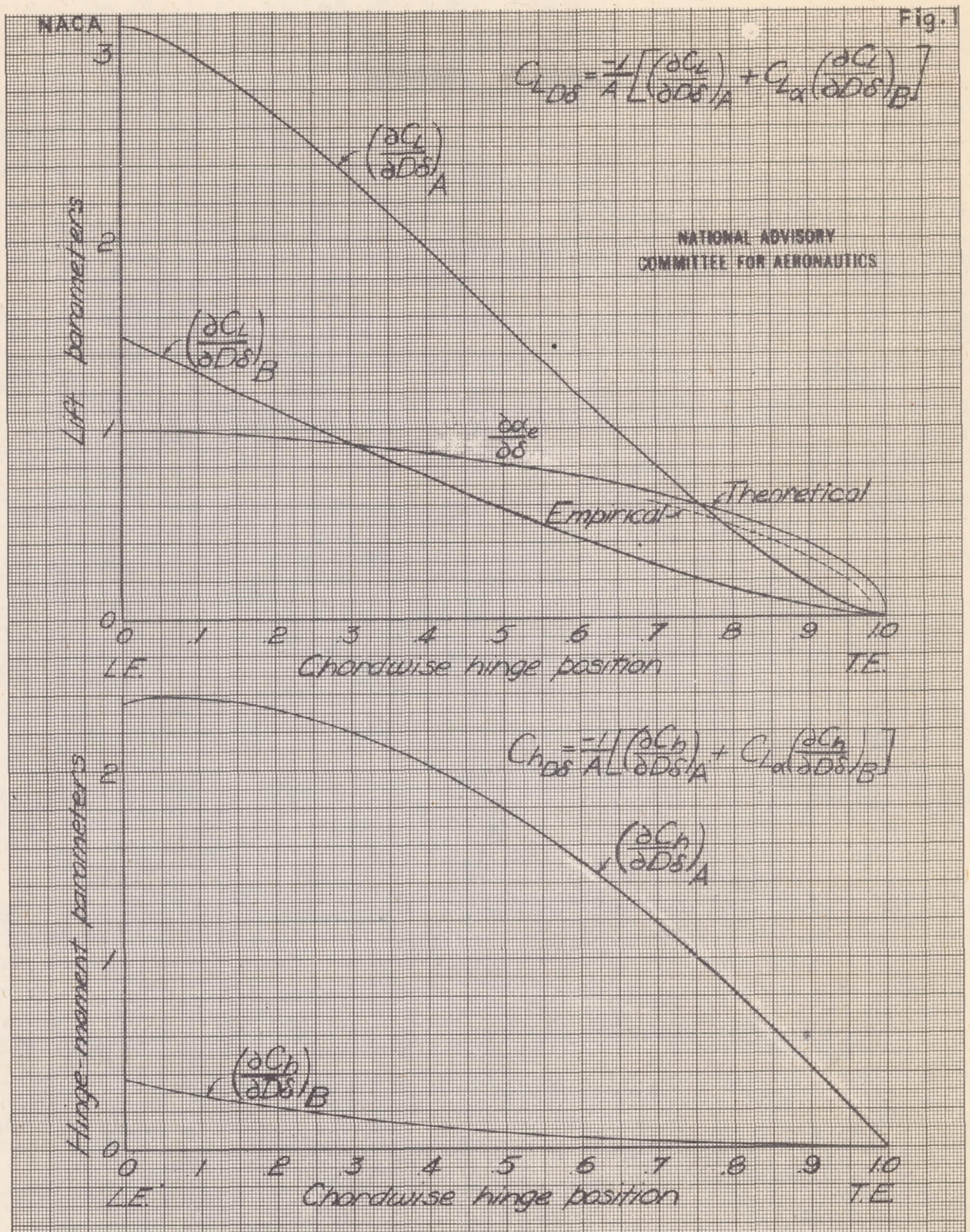

Figure 1 - Theoretical formulas and curves for determining the aerodynamic effects of angular velocity of the ailerons, derived from the equations of reference 2 for unbalanced flaps. Empirical curve for $\partial\alpha_e/\partial\delta$ from wind tunnel tests.

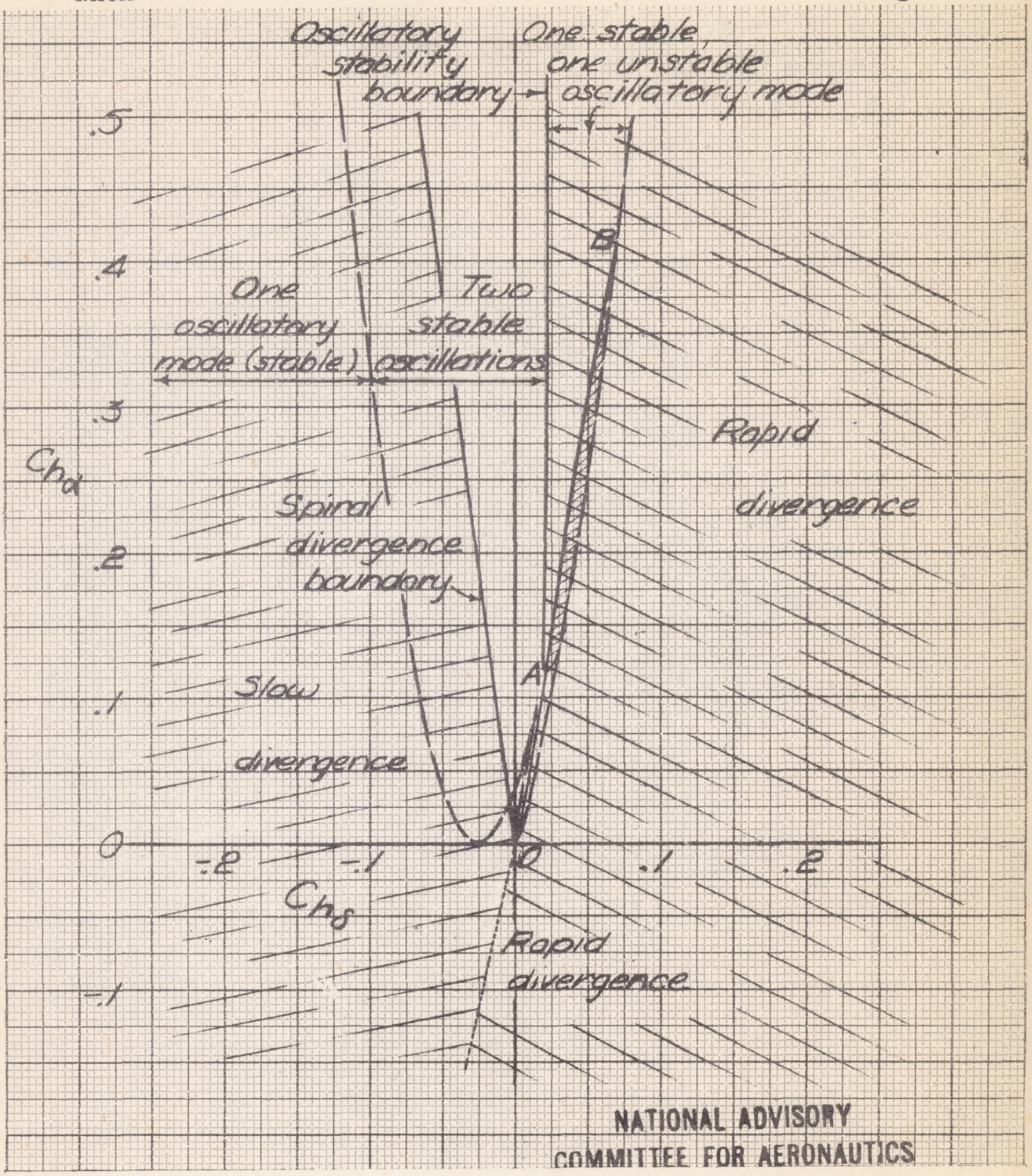

Figure 2.- Character and stability of the components of the motions found by solution of the equations before the elimination of sideslipping and yawing. (Shading indicates the unstable region.) Aileron chord, 15-percent airfoil chord; $\xi = 0$; $I_a = 0$; dihedral angle, 5°; $C_L = 1.0$.

L-361

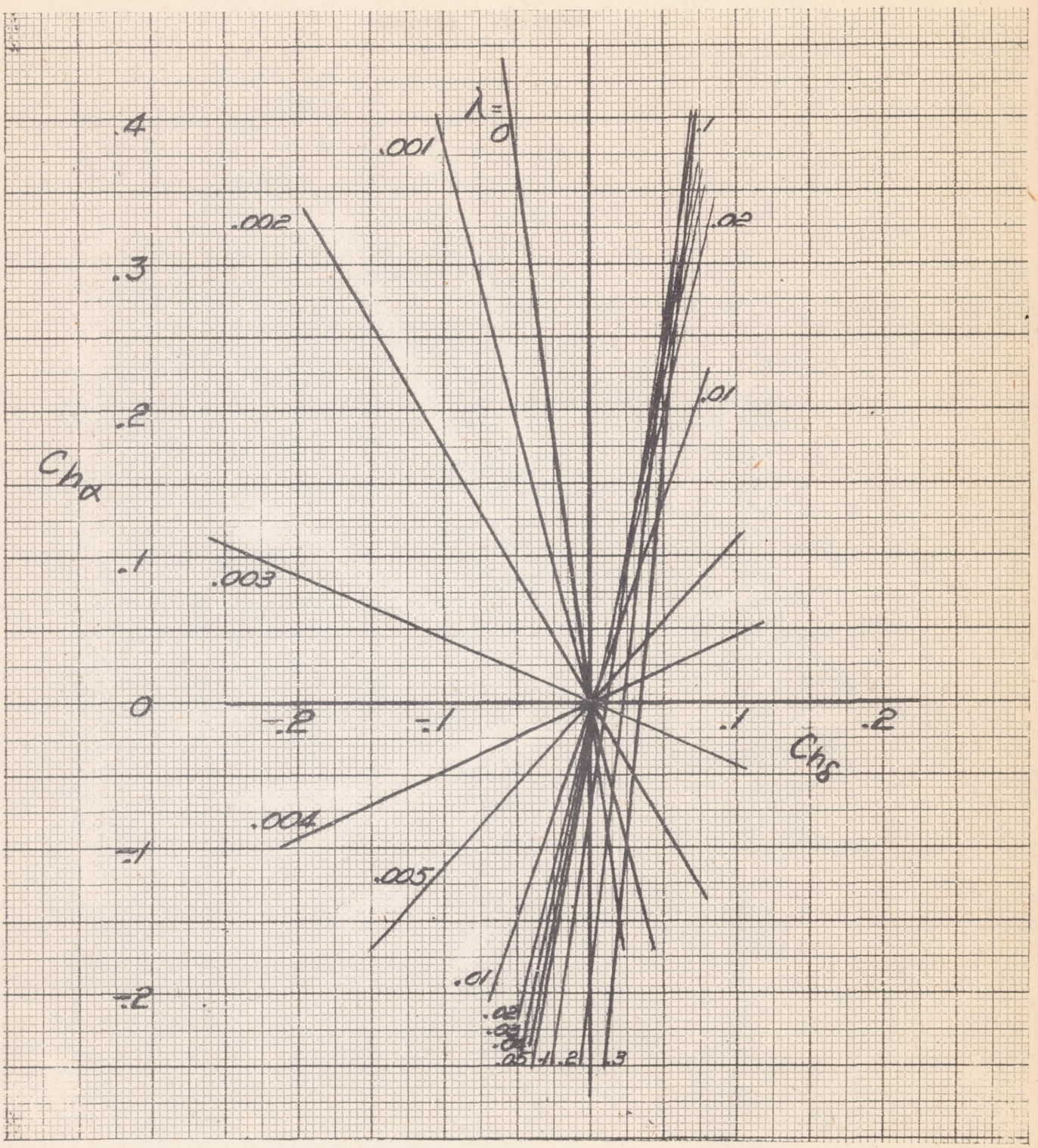

Figure 3.- Rate of divergence, as indicated by the value of the positive real roots of the stability equation. Aileron chord, 15-percent airfoil chord; $\xi = 0$; $I_a = 0$; dihedral angle, 5° ; $C_L = 1.0$.

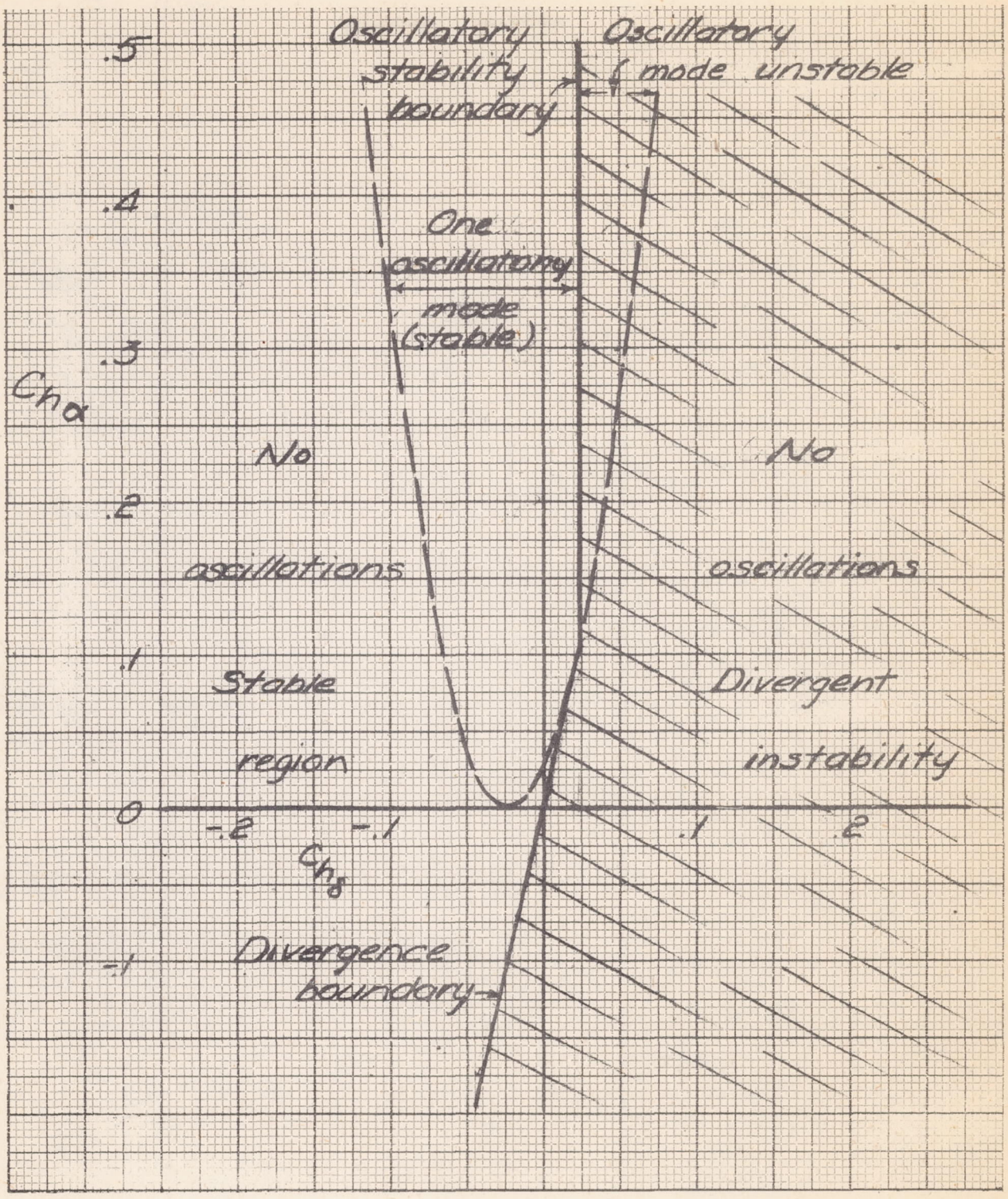

Figure 4.- Character and stability of the components of the motions with coupling only between aileron movements and rolling angle. Aileron chord, 15-percent airfoil chord; $\xi = 0$; $I_a = 0$.

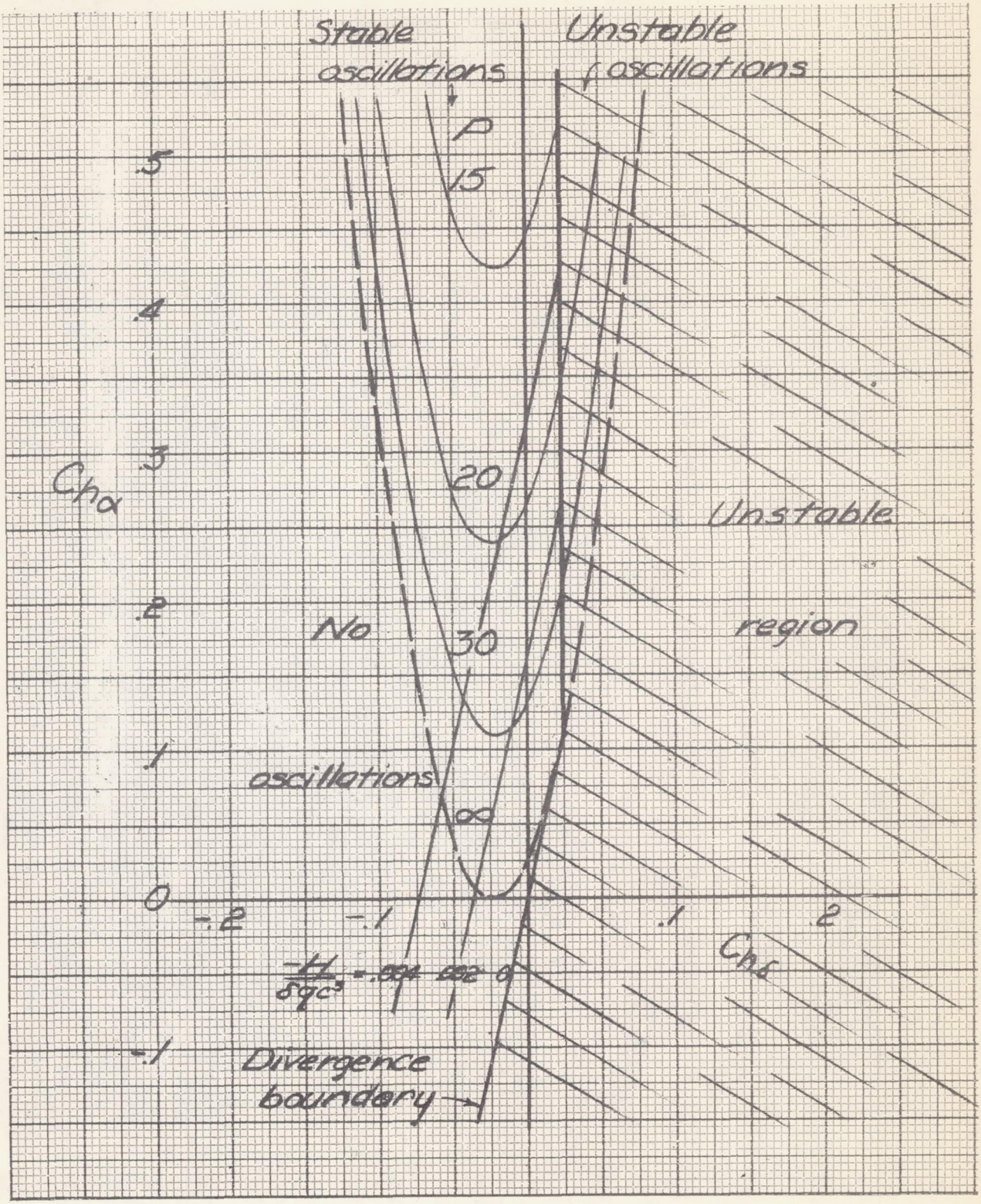

Figure 5.- Stability boundaries, lines of equal period, and lines of equal stick force for 15-percent-chord ailerons. $\xi = 0$; $I_a = 0$. Period P is in wing semispans.

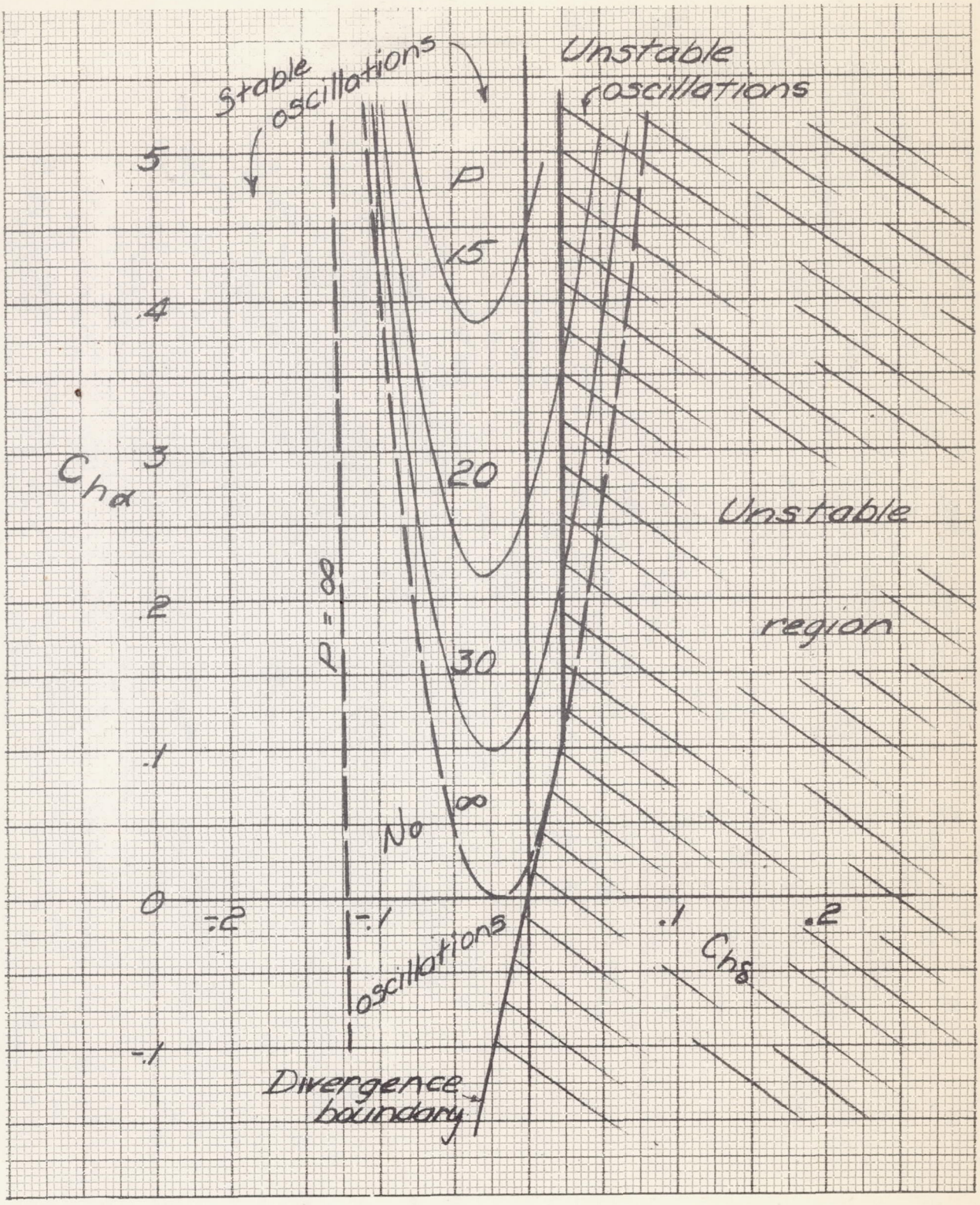

Figure 6.- Stability boundaries and lines of equal period for 15-percent-chord ailerons. $\xi = 0$; $I_a = 0.0125$. Period P is in wing semispans.

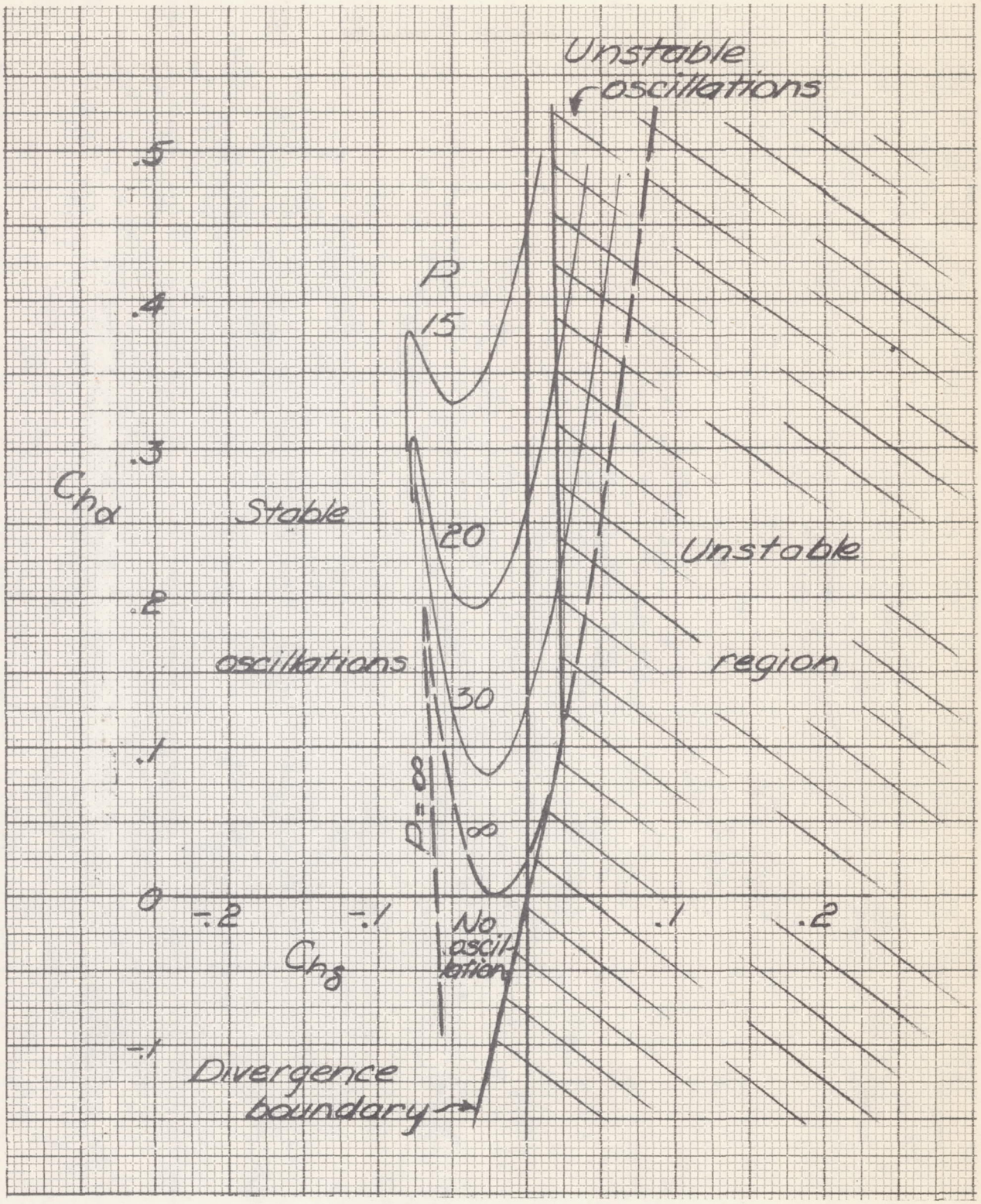

Figure 7.- Stability boundaries and lines of equal period for 15-percent-chord ailerons. $\xi = 0$; $I_a = 0.025$. Period P is in wing semispans.

L-361

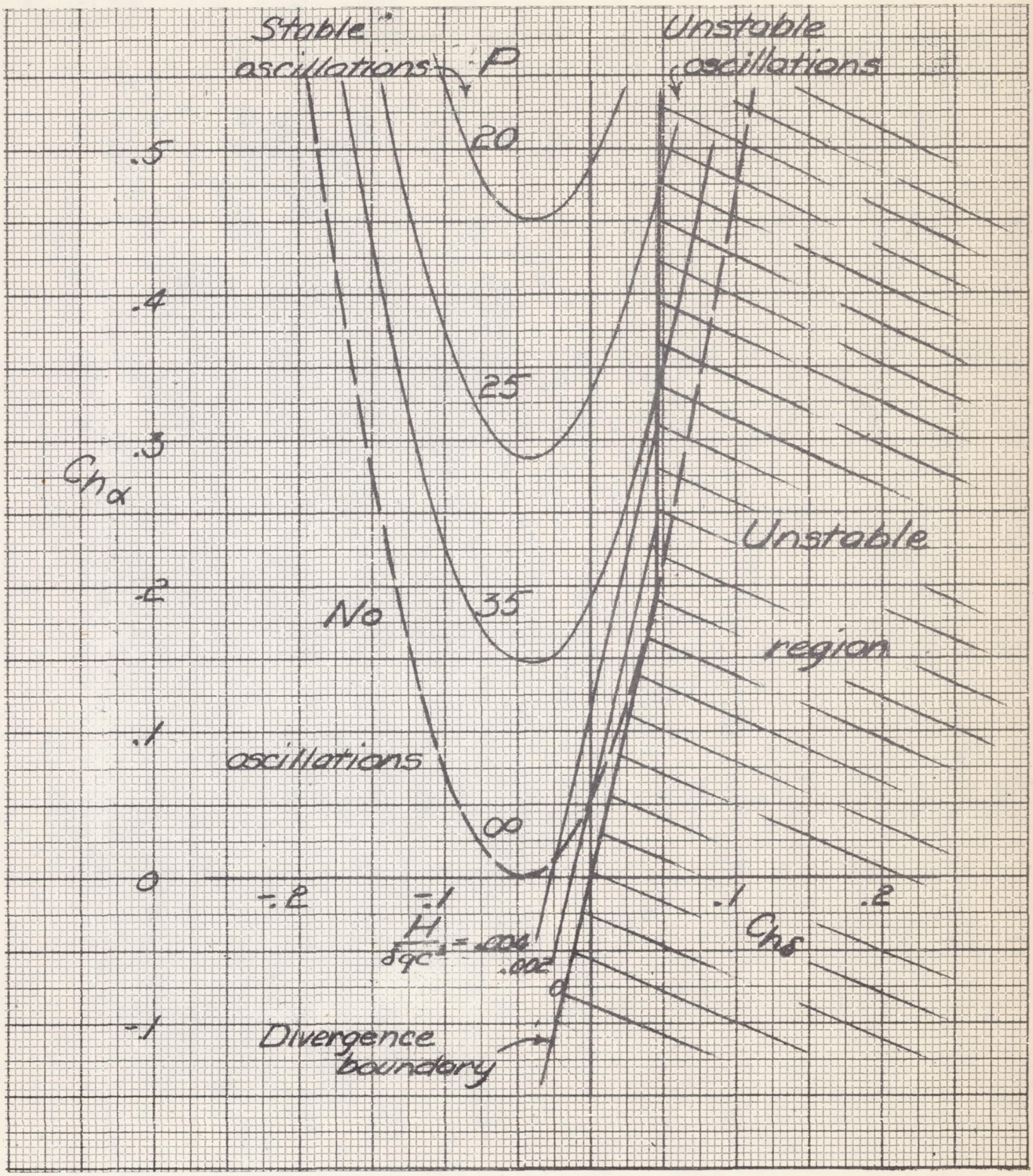

Figure 8.- Stability boundaries, lines of equal period, and lines of equal stick force for 30-percent-chord ailerons. $\xi = 0$; $I_a = 0$. Period P is in wing semispans.

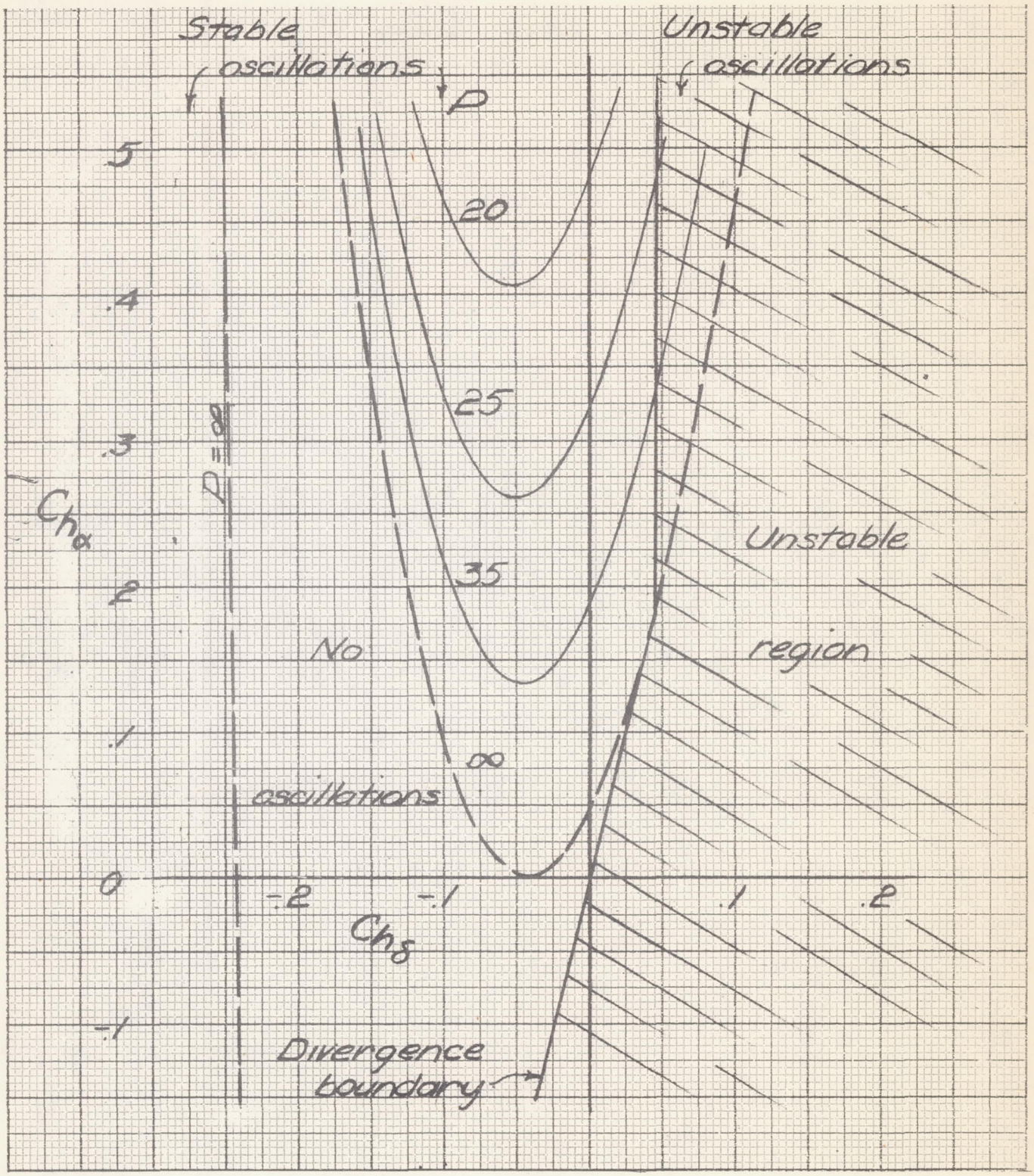

Figure 9.- Stability boundaries and lines of equal period for 30-percent-chord ailerons. $\xi = 0$; $I_a = 0.025$. Period P is in wing semispans.

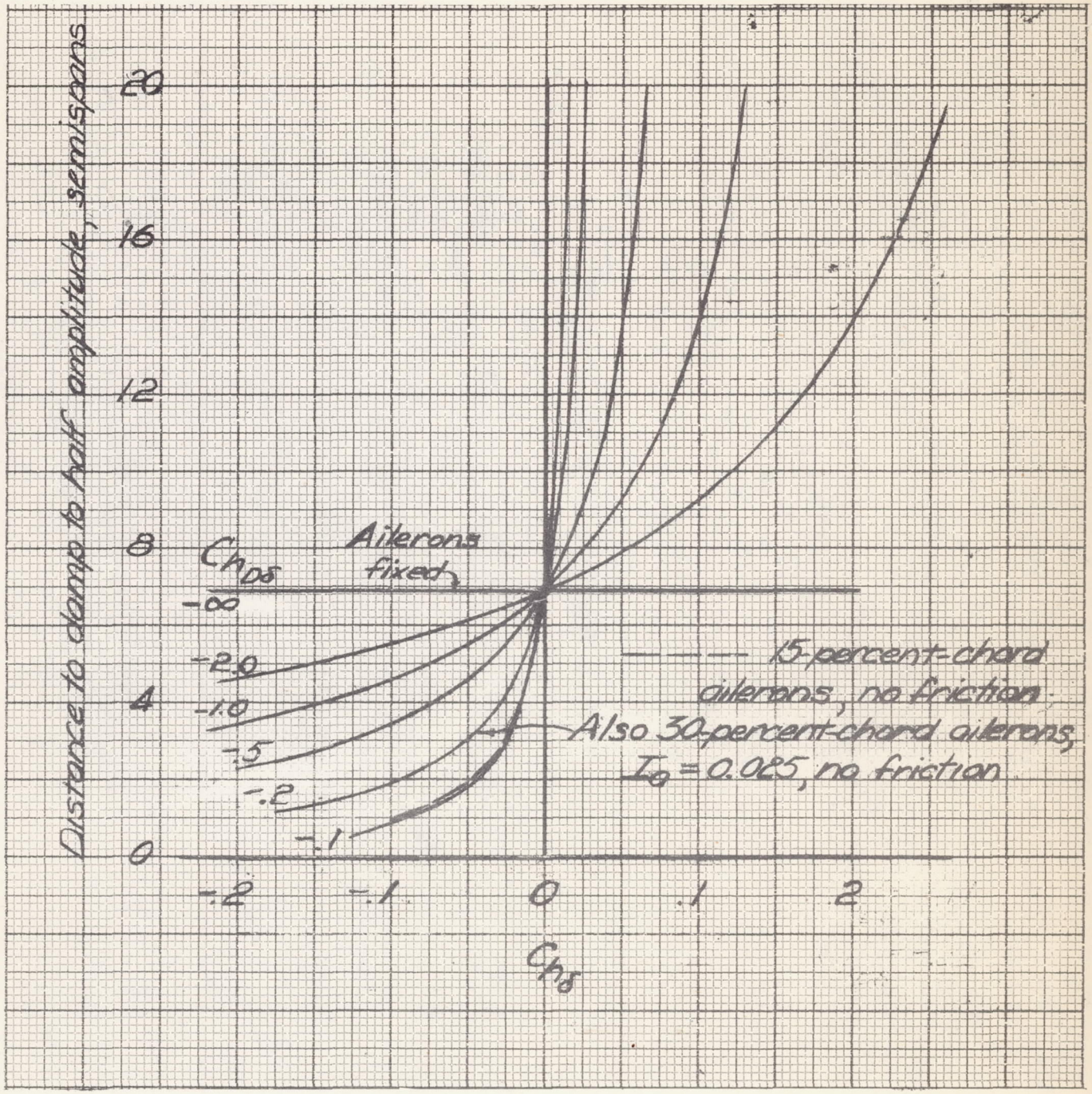

Figure 10.- Damping of the oscillations measured by the distance required to damp to half amplitude, in wing semispans, for ailerons with various values of $C_{h_{D\delta}}$. Mass-balanced ailerons, $I_a = 0.0125$; $C_{l_p}/I_X = -0.4$.

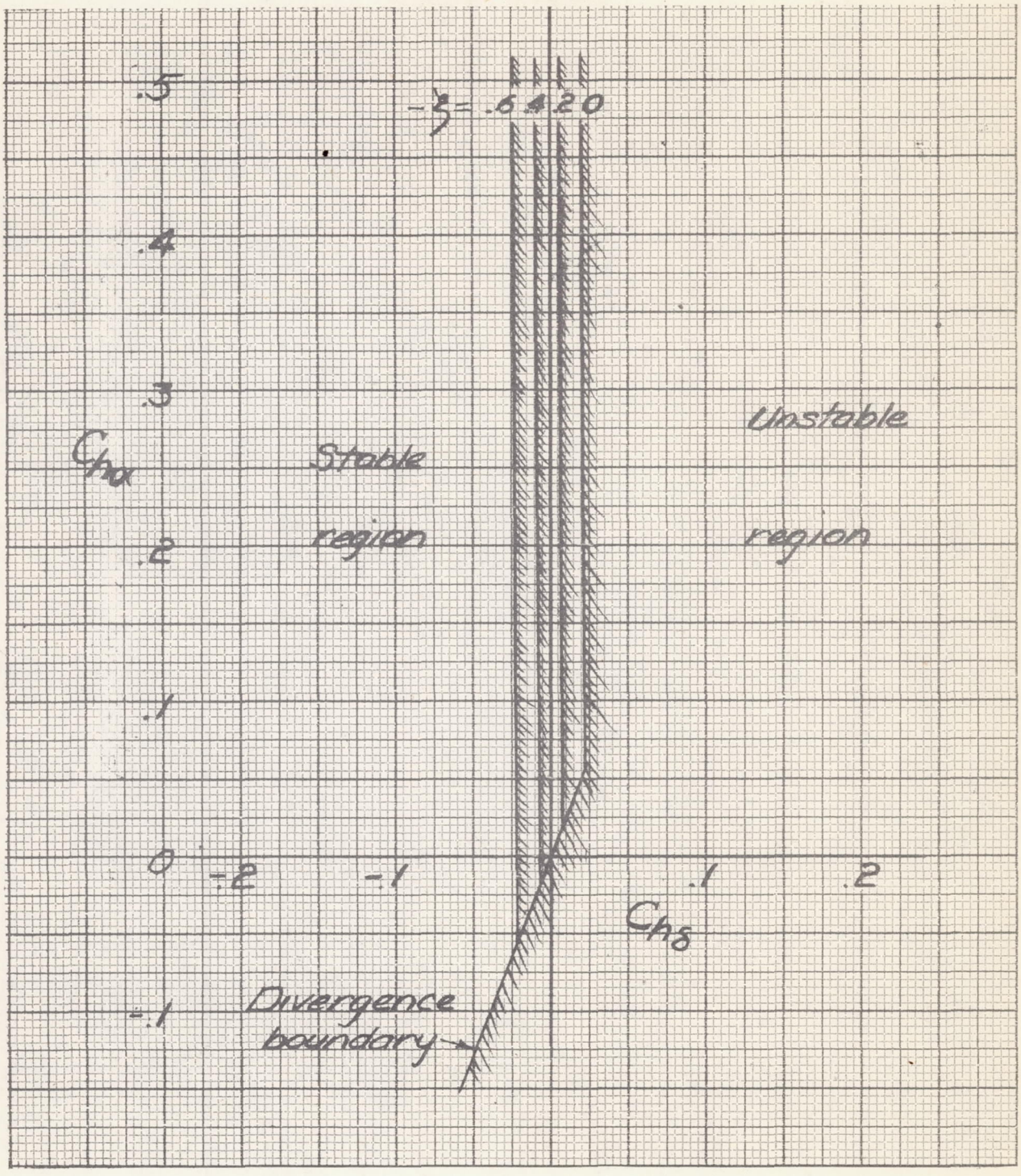

Figure 11.- Stability boundaries for 15-percent-chord ailerons, showing the effect of variation in the mass-moment parameter ξ. $I_a = 0.0125$; $C_{h_{D\delta}} = -0.011$.